Kara and Mary, International Advanced Researches and Engineering Journal 02(01): 027-032, 2018

Available online at www.dergipark.gov.tr

INTERNATIONAL ADVANCED RESEARCHES
and
ENGINEERING JOURNAL

Journal homepage: www.dergipark.gov.tr/iarej

e-ISSN: 2618-575X

International Open Access

Volume 02
Issue 01

April, 2018

Research Article

Feedback-based IKP solution with SMC for robotic manipulators: the SCARA example

Tolgay Kara[a]*, Ali Hussien Mary[b]

[a]*Department of Electrical and Electronics Engineering, University of Gaziantep, Gaziantep, Turkey*
[b]*Mechatronics Engineering Department, Al-Khwarizmi College of Engineering, University of Baghdad, Baghdad, Iraq*

ARTICLE INFO

Article history:
Received 26 February 2018
Revised 20 March 2018
Accepted 22 March 2018

Keywords:
Inverse kinematics problem
Multi-link robotic manipulators
SCARA robot

ABSTRACT

This paper presents a novel scheme for solving inverse kinematics problem (IKP) of a multi-link robotic manipulator. Important features of the proposed strategy are generality and simplicity regardless of the number of degrees of freedom (DOF) and geometry of the robot. The proposed method is a feedback strategy where the IKP solution is expressed as a dynamic control system whose goal is to maintain satisfactory trajectory tracking. As a simulation test to reveal the performance of proposed scheme, a four DOF Selective Compliance Assembly Robot Arm (SCARA) system is considered. Feedback law in proposed closed-loop solution method is selected as a combination of Sliding Mode Control (SMC) and Proportional-Derivative (PD) control for providing simplicity and robustness. Simulation results are used to show the efficacy of proposed IKP solution approach in comparison with commonly used neural networks (NN) based IKP solution method. Results reveal that proposed method yields the solution of IKP with satisfactory performance.

1. Introduction

Although different methods have been introduced to solve the IKP, still there are some weak points in these methods [1-3]. In recent years, many computational intelligence methods including NN based methods have been proposed and applied successfully for solving IKP faster than numerical methods [4-6]. Especially NN methods have been extensively preferred by researchers to solve the IKP [6-10]. Ability of fuzzy logic in modeling complex systems by generating rules based on human experiences motivated many researchers to use fuzzy logic with NN to reduce computation time required in training stage [11]. The methods mentioned above suffer from long computational time, complex computations and sensitivity to initial values.

A novel approach for the solution of the IKP is proposed in this study with a feedback structure in nature. In this approach, a feedback control system is considered where the set point is designated as the desired end-effector trajectory and the controlled variables are the joint trajectories. The solution of the IKP is achieved using a robust strategy based on PD and SMC.

2. Proposed Inverse Kinematics Solution

In this section, a novel method for solving IKP of the multi-link robotic arm based on SMC is presented. Drawbacks and disadvantages of important schemes such as NN and Jacobian based methods have been eliminated. Huge training dataset, and singularity are main drawbacks of NN and Jacobian based methods, respectively. The proposed method is a feedback strategy and for a known end effector position and orientation, a hybrid controller combining SMC with PD is proposed to minimize the error between desired and actual trajectories.

Important advantages of proposed method are:

- It is an on-line algorithm, which means it can be applied in real time.
- The solution is given in position level while most other methods are based on velocity and acceleration

* Corresponding author. Tel.: +90-342-317-2135; Fax: +90-342-360-1103.
E-mail address: kara@gantep.edu.tr

Note: This study was presented at International Advanced Researches and Engineering Congress 2017 (IAREC'17)

trajectories, which may be not be accurate due to measurement noise.

- Singularity problem is solved because proposed solution avoids determining inverse of Jacobian matrix.

SCARA robotic manipulator is used in simulations to demonstrate the effectiveness and generality of the proposed method.

2.1 Kinematic Analysis of SCARA Robot

The SCARA robotic manipulator is one of the most important and well-known robotic manipulators used successfully in many industrial applications such as packaging, cell manufacturing lines assembly, pick-and-place and so on. Figures 1 and 2 show the diagram of a 4-DOF SCARA robot in three dimensional (3D) and two dimensional (2D) views, respectively. In forward kinematics the end effector of robot arm motion with respect to the global coordinate system is studied. The origin of the global frame is located at the base of the robot arm as shown in Figure 3. Homogeneous transformation known as Denavit–Hartenberg (DH) notation is used to describe the forward kinematics of robot arm based on four parameters of each link as follows:

$$A_i = Rot(z,\theta_i)Trans(0,0,d_i)Trans(a_i,0,0)Rot(x,\alpha_i) = \begin{bmatrix} \cos\theta_i & -\sin\theta_i\cos\alpha_i & \sin\theta_i\sin\alpha_i & a_i\cos\theta_i \\ \sin\theta_i & -\cos\theta_i\cos\alpha_i & -\cos\theta_i\sin\alpha_i & a_i\sin\theta_i \\ 0 & \sin\alpha_i & \cos\alpha_i & d_i \\ 0 & 0 & 0 & 1 \end{bmatrix} \quad (1)$$

where θ_i represent joint angles from the X_{i-1} axis to the X_i about the Z_{i-1}, d_i refer to the distance between origin of the i[th] coordinate frame to the intersection of the Z_{i-1} axis along the Z_{i-1} axis, a_i represent the distance form intersection of the Z_{i-1} axis with the X_i axis to the origin of the i[th] frame along the X_i axis, and α_i are the angles from the Z_{i-1} axis to the Z_i axis about the X_i [12]. DH parameters of the SCARA robot are shown in Table 1.

Table 1. DH parameters of SCARA robot

i	q_i	d_i	a_i	α_i
1	q_1	L_{12}	L_{11}	0
2	q_2	0	L_2	0
3	0	d_3	0	π
4	q_4	L_4	0	0

$$A_{end-effector} = A_1.A_2.A_3.A_4 = \begin{bmatrix} n_x & s_x & a_x & p_x \\ n_y & s_y & a_y & p_y \\ n_z & s_z & a_z & p_z \\ 0 & 0 & 0 & 1 \end{bmatrix} \quad (2)$$

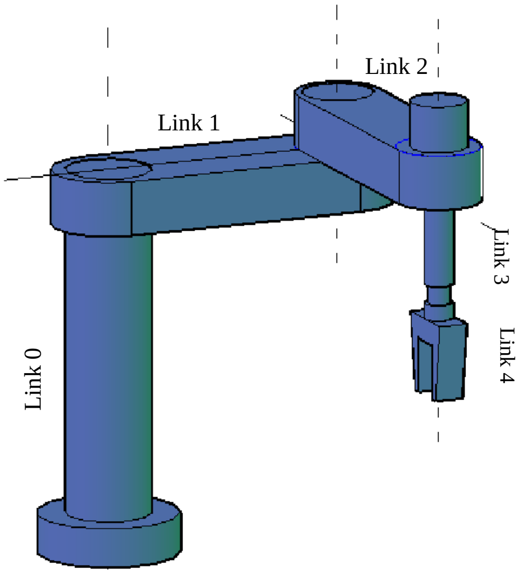

Figure 1. 3D view of the SCARA system

$$A_1 = \begin{bmatrix} \cos\theta_1 & -\sin\theta_1 & 0 & L_{11}\cos\theta_1 \\ \sin\theta_1 & -\cos\theta_1 & 0 & L_{11}\sin\theta_1 \\ 0 & 0 & 1 & L_{12} \\ 0 & 0 & 0 & 1 \end{bmatrix} \quad (3)$$

$$A_2 = \begin{bmatrix} \cos\theta_2 & -\sin\theta_2 & 0 & L_2\cos\theta_2 \\ \sin\theta_2 & \cos\theta_2 & 0 & L_2\sin\theta_2 \\ 0 & 0 & 1 & 0 \\ 0 & 0 & 0 & 1 \end{bmatrix} \quad (4)$$

$$A_3 = \begin{bmatrix} 1 & 0 & 0 & 0 \\ 0 & -1 & 0 & 0 \\ 0 & 0 & -1 & d_3 \\ 0 & 0 & 0 & 1 \end{bmatrix}, \quad (5)$$

$$A_4 = \begin{bmatrix} \cos\theta_4 & -\sin\theta_4 & 0 & 0 \\ \sin\theta_2 & \cos\theta_2 & 0 & 0 \\ 0 & 0 & 1 & L_2 \\ 0 & 0 & 0 & 1 \end{bmatrix}, \quad (6)$$

$$A_{end-effector} = \begin{bmatrix} \cos\theta_{124} & \sin\theta_{124} & 0 & L_2\cos\theta_{12} + L_{11}\cos\theta_1 \\ \sin\theta_{124} & -\cos\theta_{124} & 0 & L_2\sin\theta_{12} + L_{11}\sin\theta_1 \\ 0 & 0 & -1 & L_{12} + d_3 - L_4 \\ 0 & 0 & 0 & 1 \end{bmatrix} \quad (7)$$

where a short notation for trigonometric functions is used in (7) such as: $\cos\theta_{ijk}$ stands for $\cos(\theta_i + \theta_j - \theta_k)$, and $\cos\theta_{ij}$ stands for $\cos(\theta_i + \theta_j)$, etc. The end effector orientation can be described based on of the roll-pitch-yaw (RPY) rotations [12, 13]. The rotational angles around the X, Y, and Z axes are:

$$RPY(\varphi_x,\varphi_y,\varphi_z) = Rot(Z_0,\varphi_z)Rot(Y_0,\varphi_y)Rot(X_0,\varphi_x) = \begin{bmatrix} C_{\varphi_y}C_{\varphi_z} & S_{\varphi_x}S_{\varphi_y}C_{\varphi_z} - C_{\varphi_x}S_{\varphi_z} & C_{\varphi_x}S_{\varphi_y}C_{\varphi_z} - S_{\varphi_x}S_{\varphi_z} \\ C_{\varphi_y}S_{\varphi_z} & S_{\varphi_x}S_{\varphi_y}C_{\varphi_z} - C_{\varphi_x}C_{\varphi_z} & C_{\varphi_x}S_{\varphi_y}S_{\varphi_z} - S_{\varphi_x}C_{\varphi_z} \\ -S_{\varphi_y} & S_{\varphi_x}C_{\varphi_y} & C_{\varphi_x}C_{\varphi_y} \end{bmatrix} \quad (8)$$

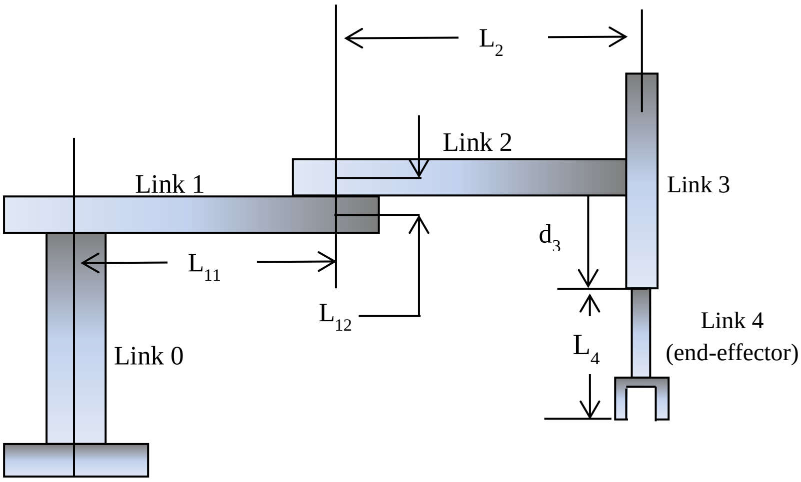

Figure 2. 2D diagram of the SCARA system

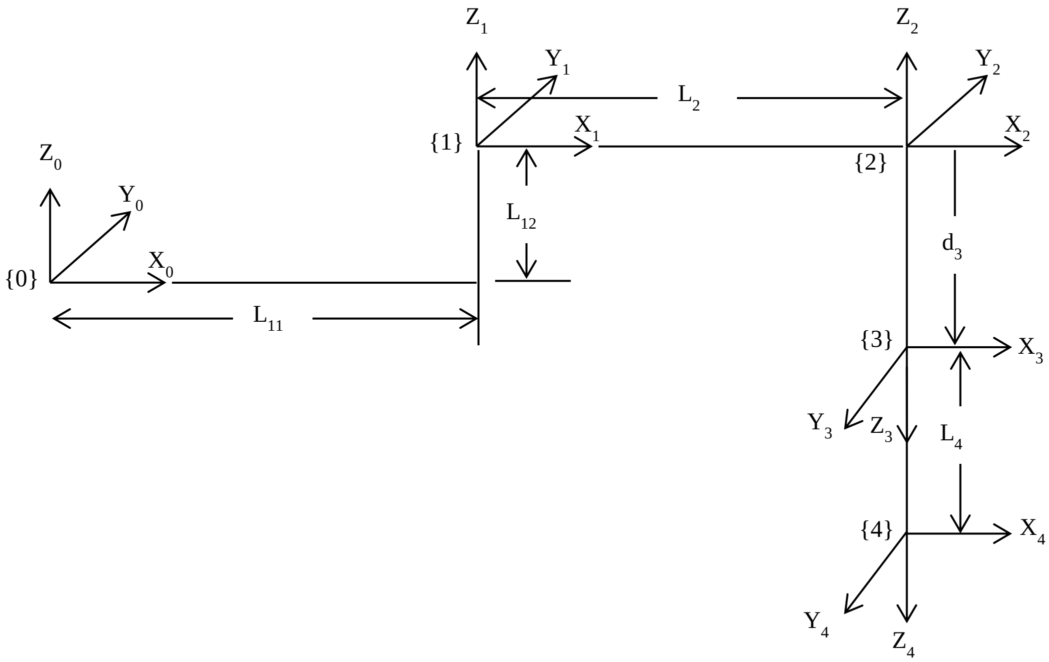

Figure 3. Frame assignment of SCARA system

These angles can be obtained by comparing (7) with the expression in (8).

$$\varphi_x = 0, \quad (9)$$
$$\varphi_y = \pi, \quad (10)$$
$$\varphi_z = \theta_{124}. \quad (11)$$

The forward kinematic of SCARA robot arm can be expressed as:

$$(X, Y, Z, \varphi_z) = F_{Fk}(\theta_1, \theta_2, d_3, \theta_4), \quad (12)$$

and the inverse kinematic for SCARA robot arm is:

$$(\theta_1, \theta_2, d_3, \theta_4) = F_{Ik}\ (X, Y, Z, \varphi_z). \quad (13)$$

2.2 Proposed Robust IKP Solution

The proposed technique for solving the IKP based on feedback theory with SMC by restating the IKP as a dynamic control problem is shown in Figure 4. The proposed method uses the desired Cartesian space trajectory as reference, and the control goal is to find a joint trajectory that can track the desired one. Desired input is the variables in Cartesian space $x_d = [X\ Y\ Z\ \varphi_z]$ while the output is the variables in joint space $\theta = [\theta_1\ \theta_2\ d_3\ \theta_4]$. The proposed method overcomes the drawbacks of previous methods that have been suggested to solve the IKP like complex computations, singularity problem and long time required in iteration methods as discussed above. The proposed control law for this tracking problem is:

$$u = u^{PD} + u^{smc}, \quad (14)$$
$$u^{PD} = k_p\, e(t) + k_d \dot{e}(t), \quad (15)$$
$$u^{smc} = Hsat(s, \emptyset), \quad (16)$$
$$e(t) = x_d(t) - x(t), \quad (17)$$
$$\dot{e}(t) = \dot{x}_d(t) - \dot{x}(t), \quad (18)$$
$$s(t) = \beta e(t) + \dot{e}(t), \quad (19)$$

where $e(t)$ represents the difference between the current and the desired Cartesian coordinates. Using saturation function for switching as given in (16) is a well-established technique in literature [14-16]. Here we propose combination of this technique with the conventionally used PD type sliding surface given in (15) [17, 18].

Remark: The control law depends only on the error signal, its derivative, and the sliding surface. As a consequence, proposed technique is applicable to all kinds of robotic manipulators.

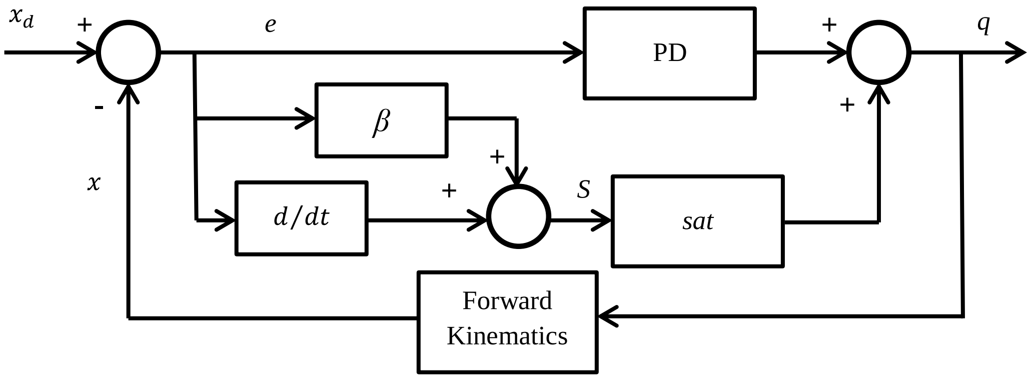

Figure 4. Block diagram of proposed robust IK solution

3. Simulation Tests

The performance of proposed method that is based on PD control with SMC for solving IKP is discussed in this section. In order to demonstrate effectiveness of the proposed IK solution scheme, computer simulation is used for solving IKP of SCARA robot. Performance of proposed method is compared with NN method, which has been used widely in solving IKP in recent years. Since the NN methods are offline, at first they must be trained to learn the map between variables in joint space and variables in Cartesian space. The values of DH parameters used in this simulation are as follows: $L_{11} = 1$, $L_{12} = 0.1$, $L_2 = 1$, and $L_4 = 1$. The gain parameters of proposed controller are $k_p = H = 500 I_4$, $k_d = 10 I_4$, $\emptyset = 0.01$. The following desired trajectory is used in this simulation:

$$x_d(t) = \cos\left(\frac{\pi}{3} + 0.1\sin(7t)\right) + \cos\left(\frac{\pi}{2} + 0.1\sin(7t) + 0.1\cos(t)\right) \quad (20)$$
$$y_d(t) = \sin\left(\frac{\pi}{3} + 0.1\sin(7t)\right) + \sin\left(\frac{\pi}{2} + 0.1\sin(7t) + 0.1\cos(t)\right) \quad (21)$$
$$z_d(t) = 1 + 0.1t. \quad (22)$$

Note that the tracking control is applied for a maximum simulation time of 10 seconds, which limits the motion along Z direction between 1 and 2. For practical implementation and longer simulation times, the reference trajectory in Z direction should be limited. Figure 5 shows the desired path of end effector in Cartesian space. Integral of the absolute value of the error (IAE) is used for comparison:

$$IAE = \int_0^{tf} |e(t)| dt. \quad (23)$$

Therefore the error along X, Y and Z axes can be determined as follows:

$$Err_x = \int_0^{tf} |e_x(t)| dt = \int_0^{tf} |x(t) - x_d(t)| dt \quad (24)$$
$$Err_y = \int_0^{tf} |e_y(t)| dt = \int_0^{tf} |y(t) - y_d(t)| dt \quad (25)$$
$$Err_z = \int_0^{tf} |e_z(t)| dt = \int_0^{tf} |z(t) - z_d(t)| dt. \quad (26)$$

Roll angle which represents orientation of the end effector is shown in Figure 6 and Cartesian space errors along the X, Y and Z axes are shown in Figure 7. As expected because the trajectory along Z axis is based only on d_3, the NN can easily approximate this relation therefore neural network method and also the proposed control method have very small error value in this axis. These results indicate clearly high accuracy of proposed method. Moreover, proposed method is an on-line method. Performance indices listed in Table 2 indicate superiority of proposed method, where the IAE values are very small for X and Y directions, and almost equal to zero in Z direction. Therefore, the actual Cartesian path is very close to desired Cartesian path with very small cumulative error.

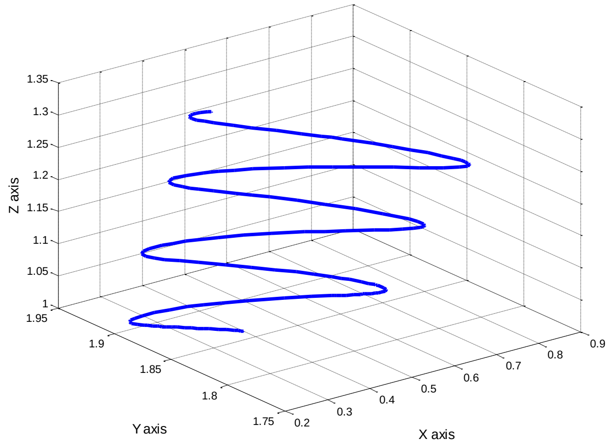

Figure 5. Desired trajectory in Cartesian space

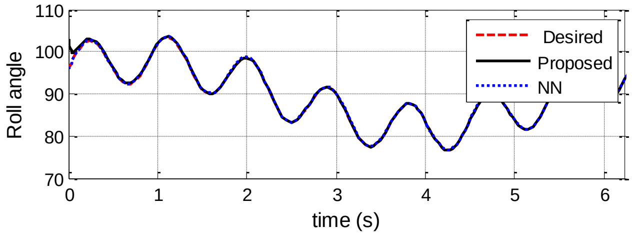

Figure 6. Variation of roll angle versus time

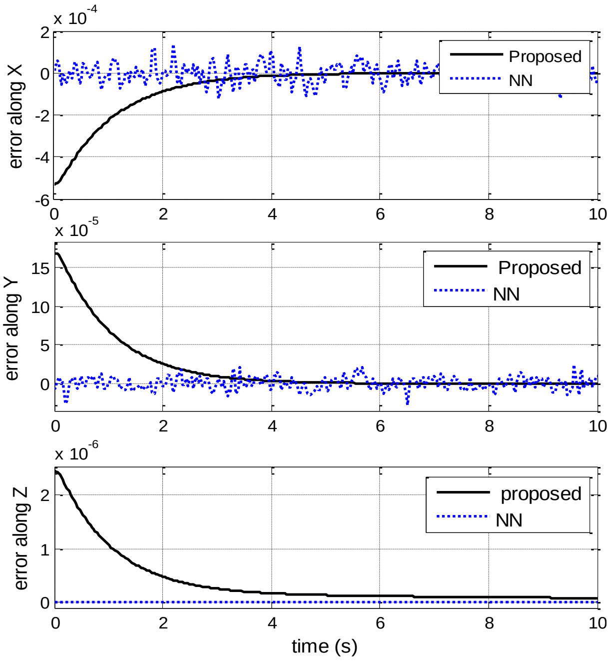

Figure 7. Variation of roll angle along Cartesian axes

Table 2. Performance index IAE values for three Cartesian axes

	Proposed	**NN**
Err_x	0.0014	0.0097
Err_y	0.0020	0.0048
Err_z	~0	~0

4. Conclusion

In this paper, a novel IKP solution method for multi-link robotic manipulators based on a feedback control strategy is proposed. The method relies on tracking control with a desired trajectory that represents the desired end-effector angle variation. Proposed method is independent from the degrees of freedom of the manipulator and it is applicable to all kinds of robotic manipulators. A robust scheme that combines PD and SMC is used in the feedback control law. Performance of the method in solving IKP of a SCARA system is illustrated via simulation test results in comparison with the common NN based IKP solution approach. Results prove applicability of proposed method with satisfactory performance.

References

1. Alavandar, S., and M. J. Nigam, *Inverse kinematics solution of 3DOF planar robot using ANFIS.* Int. J. of Computers, Communications & Control, 2008. **3:** p. 150-155.
2. Shen, W, J. Gu, and E. E. Milios, *Self-configuration fuzzy system for inverse kinematics of robot manipulators*, in IEEE Annual meeting of the North American Fuzzy Information Processing Society NAFIPS 2006: p. 41-45.
3. Tarokh, Mahmoud, and M. Kim, *Inverse kinematics of 7-DOF robots and limbs by decomposition and approximation.* IEEE transactions on robotics, 2007. **23**(3): p. 595-600.
4. Duka, A. V., *ANFIS based Solution to the Inverse Kinematics of a 3 DOF planar Manipulator.* Procedia Technology, 2015. **19**: p. 526-533.
5. Duka, A. V., *Neural network based inverse kinematics solution for trajectory tracking of a robotic arm.* Procedia Technology, 2014. **12**: p. 20-27.
6. Ma, C., Z. Yong, C. Jin., W. Bin, and Z. Qinjun, *Inverse kinematics solution for 6R serial manipulator based on RBF neural network.* In International Conference on Advanced Mechatronic Systems ICAMechS 2016: p. 350-355.
7. Mayorga, R. V., and P. Sanongboon, *Inverse kinematics and geometrically bounded singularities prevention of redundant manipulators: An Artificial Neural Network approach.* Robotics and Autonomous Systems, 2005. **53**(3): p. 164-176.
8. Pérez-Rodríguez, R, M-C. Alexis, C. Ursula, S. Javier, C. Cesar, O. Eloy, M. T. Josep, M. Josep, and J. G. Enrique, *Inverse kinematics of a 6 DoF human upper limb using ANFIS and ANN for anticipatory actuation in ADL-based physical Neurorehabilitation.* Expert Systems with Applications, 2012. **39**(10): p. 9612-9622.
9. Zou, X., G. Dawei, W. Liping, and G. Zhenyu, *A novel method to solve inverse variational inequality problems based on neural networks*, Neurocomputing, 2016. **173**(3): p. 1163-1168.

10. Assal, S. F. M, W. Keigo, and I. Kiyotaka, *Neural Network-Based Kinematic Inversion of Industrial Redundant Robots Using Cooperative Fuzzy Hint for the Joint Limits Avoidance.* IEEE/ASME Transactions on mechatronics, 2016. **11**(5): p. 593-603.
11. Lazarevska, E., *A Neuro-Fuzzy Model of the Inverse Kinematics of a 4 DOF Robotic Arm,* in IEEE 14th International Conference on Modelling and Simulation UKSim2012: p. 306-311.
12. Köker, R., *Reliability-based approach to the inverse kinematics solution of robots using Elman's networks.* Engineering applications of artificial intelligence, 2005. **18**(6): p. 685-693.
13. Rolf, M. and J. J. Steil, *Efficient Exploratory Learning of Inverse Kinematics on a Bionic Elephant Trunk.* Neural Networks and Learning Systems, IEEE Transactions on, 2013. **25**(6): p. 1147-1160.
14. Slotine, J-J E., and W. Li, *Applied nonlinear control.* Vol. 199. No. 1. Englewood Cliffs, NJ: Prentice hall, 1991.
15. Fallaha, C. J., M. Saad, H. Y. Kanaan, and K. Al-Haddad, *Sliding-mode robot control with exponential reaching law*. IEEE Transactions on Industrial Electronics, 2001, **58**(2), 600-610.
16. Kachroo, P. and M. Tomizuka, *Chattering reduction and error convergence in the sliding-mode control of a class of nonlinear systems.* IEEE Transactions on Automatic Control , 1996, **41**(7): p.1063-1068.
17. Eker, I., *Sliding mode control with PID sliding surface and experimental application to an electromechanical plant.* ISA transactions, 2006, **45**(1): p.109-118.
18. Parra-Vega, V., S. Arimoto, Y. H. Liu, G. Hirzinger, and P. Akella,(2003). *Dynamic sliding PID control for tracking of robot manipulators: Theory and experiments.* IEEE Transactions on Robotics and Automation, 2003, **19**(6): p. 967-976.